Journal Pre-proof

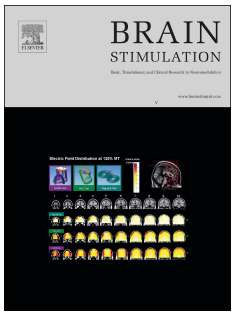

Reclassifying Transcranial Pulse Stimulation as TNUS: Nonlinear Mechanics Necessitate Departure from the ITRUSST Framework

Qinxi Luo, Neng Huang, Dan Li, Xinxin Chen, Zhu Liu, Leihao Sha, Changliang Liu, Yonghong Yang, Shizheng Wu, Lars Wojtecki, Lei Chen, Cheng Huang

PII: S1935-861X(26)00076-8

DOI: https://doi.org/10.1016/j.brs.2026.103099

Reference: BRS 103099

To appear in: *Brain Stimulation*

Received Date: 21 October 2025

Revised Date: 10 April 2026

Accepted Date: 10 April 2026

Please cite this article as: Luo Q, Huang N, Li D, Chen X, Liu Z, Sha L, Liu C, Yang Y, Wu S, Wojtecki L, Chen L, Huang C, Reclassifying Transcranial Pulse Stimulation as TNUS: Nonlinear Mechanics Necessitate Departure from the ITRUSST Framework, *Brain Stimulation*, https://doi.org/10.1016/j.brs.2026.103099.

Reclassifying Transcranial Pulse Stimulation as TNUS: Nonlinear Mechanics Necessitate Departure from the ITRUSST Framework

Qinxi Luo[1,2,3,4], Neng Huang[1,2], Dan Li[1,2], Xinxin Chen[5], Zhu Liu[6], Leihao Sha[6], Changliang Liu[4,9], Yonghong Yang[1,2], Shizheng Wu[4], Lars Wojtecki[7,8], Lei Chen[4,6], Cheng Huang[1,2,4*]

Affiliations

1. Department of Rehabilitation Medicine, West China Hospital, Sichuan University, No. 37 Guoxue Alley, Chengdu, 610041, Sichuan, China

2. Key Laboratory of Rehabilitation Medicine in Sichuan Province, West China Hospital, Sichuan University, No. 37 Guoxue Alley, Chengdu, 610041, Sichuan, China

3. School of Rehabilitation Sciences, West China School of Medicine, Sichuan University, No. 37 Guoxue Alley, Chengdu, 610041, Sichuan, China

4. Center for High Altitude Medicine, West China Hospital, Sichuan University, No. 37 Guoxue Alley, Chengdu, 610041, Sichuan, China

5. Department of Rehabilitation Medicine, The First Affiliated Hospital, Sun Yat-sen University, No. 58 Zhongshan Road 2, Guangzhou, 510080, Guangdong, China

6. Department of Neurology, West China Hospital, Sichuan University, No. 37 Guoxue Alley, Chengdu, 610041, Sichuan, China

7. Department of Neurology and Neurorehabilitation, Hospital zum Heiligen Geist GmbH & Co.KG, Academic Teaching Hospital of the Heinrich-Heine-University Düsseldorf, Hubertusstraße 100, 47906 Kempen, Germany

8. Institute of Clinical Neuroscience & Medical Psychology, University Clinic Düsseldorf, Moorenstraße 5, 40225 Düsseldorf, Germany

9. High Altitude Medicine Key Laboratory of Sichuan Province, Institute of High-Altitude Medicine, West China Hospital, Sichuan University, No. 37 Guoxue Alley, Chengdu, Sichuan 610041, China

*Corresponding author: Cheng Huang; Full address: 37 Guoxue Lane, Wuhou District, Chengdu, Sichuan Province, People's Republic of China,610041

E-mail: chenghuang_scu@163.com

Abstract

Background: Transcranial ultrasound has emerged as a promising non-invasive neuromodulation modality for Alzheimer's disease (AD). However, its clinical translation is hindered by inconsistent biophysical classification between quasi-linear low-intensity focused ultrasound (LIFU) and nonlinear pulse-based approaches.

Objective: To propose a Transcranial Nonlinear Ultrasound Stimulation (TNUS) framework for the formal reclassification of Transcranial Pulse Stimulation (TPS), enabling clear differentiation of nonlinear wave mechanics from quasi-linear acoustics.

Methods: This perspective review integrates biophysical modeling within the nonlinear Westervelt regime, critically appraises recent clinical trial data, and conducts a comparative

analysis of acoustic dosimetry by contrasting the periodic waves characteristic of linear LIFU with the shock-front dynamics of TPS.

Results: TPS is characterized by an extreme pressure gradient ($dP/dt \approx 10^{13}$ Pa/s), representing a five-order-of-magnitude divergence from LIFU. This regime facilitates a Volume Force model and Ballistic Gating of ion channels via displacement currents, a mechanism distinct from the steady-state pathways of intramembrane cavitation. In the atrophied AD brain, pathological expansion of the cerebrospinal fluid (CSF) compartment induces focal displacements and compromises wavefront integrity through refractive aberrations at the CSF–parenchyma interface. While the Glassy Regime of tissue provides a biomechanical safety buffer, the compromised compliance in Cerebral Amyloid Angiography (CAA) requires TPS protocols to remain below the vascular ultimate tensile strength (UTS).

Conclusions: Future clinical optimization of TPS necessitates a transition toward structure-aware dosimetry. The implementation of adaptive beamforming (e.g., TUSNet) and individualized impulse titration is essential to mitigate refractive aberrations and vascular failure risks in the pathologically heterogeneous aging brain.

Key words

Alzheimer's Disease; Dementia; Low-intensity focused ultrasound; Transcranial pulse stimulation; Transcranial focused ultrasound stimulation

1. Introduction

The therapeutic landscape for Alzheimer’s disease (AD) remains at a pivotal juncture. While amyloid-beta ($A\beta$) monoclonal antibodies have secured regulatory approval, their

clinical utility is limited by suboptimal blood-brain barrier (BBB) penetration and modest clinical benefits in cognitive function[1,2]. This limitation has catalyzed a shift toward physical neuromodulation, with transcranial ultrasound emerging as a leading modality due to its non-invasive nature and millimetric precision[3–11].

The rapid clinical translation of transcranial ultrasound has engendered a significant methodological inconsistency (Figure 1). Current literature frequently conflates the quasi-linear periodic waves of Low-Intensity Focused Ultrasound (LIFU) with the nonlinear shockwaves characteristic of Transcranial Pulse Stimulation (TPS)[4,12–18]. This terminological ambiguity obscures a fundamental biophysical reality: the atrophied AD brain functions as an aberrating medium. The expansion of the cerebrospinal fluid (CSF) layer induces significant refractive shifts, leading to a loss of wavefront integrity before the acoustic energy reaches the targeted focus[19,20].

To achieve biophysical transparency, we propose a reclassification of TPS as Transcranial Nonlinear Ultrasound Stimulation (TNUS). Although the clinical term TPS is retained for continuity, this redefinition is essential for establishing safety and efficacy standards distinct from linear acoustics[21–25]. This review evaluates the translational gap in AD therapy across four biophysical domains: (1) the paradigm shift from steady-state acoustic radiation force to impulsive momentum transfer; (2) the technical inadequacy of linear dosimetry (I_{spta}) in strictly nonlinear regimes; (3) a mechanistic audit of recent clinical evidence; and (4) the transition toward refraction-aware, adaptive neuromodulation (see Table 1 and Table 2 for abbreviations and symbols). We aim to establish a rigorous TNUS framework to synchronize nonlinear wave mechanics with clinical neurophysiology.

2. Biophysical Reclassification: TPS as TNUS

2.1 Reclassifying TPS as TNUS

To enhance clinical precision, it is necessary to rectify a persistent methodological oversight: the classification of TPS as a conventional form of pulsed ultrasound. From the perspective of nonlinear wave mechanics, TPS is more accurately classified as TNUS[26–30]. Unlike the infinitesimal displacements characteristic of linear acoustics, TPS is governed by the nonlinear parameters of the Westervelt equation, where wave propagation is dominated by shock-front steepening[26,28,29,31,32](Figure 2). While the nomenclature "TPS" is maintained herein to ensure bibliographic continuity with current clinical literature, we propose that the underlying energy-tissue interactions are more accurately interpreted through a nonlinear framework[16,23–25,31,33,34].Consequently, we suggest the designation TNUS as a more biophysically precise descriptor for future classification. Adopting this terminology would effectively distinguish the unique impulsive physics of this modality from the mechanisms of conventional linear neuromodulation.

2.2 The Nonlinear Threshold: dP/dt vs. I_{spta}

The fundamental divergence between LIFU and TPS resides in the pressure gradient (dP/dt) and the resulting harmonic bandwidth[4,18,35–40]. LIFU typically operates within a quasi-linear regime ($dP/dt \approx 10^8$ Pa/s), where bioeffects are primarily attributed to time-averaged acoustic radiation force (ARF) under periodic oscillation[20,41–44]. In this context, the spatial-peak temporal-average intensity (I_{spta}) serves as a reliable metric for evaluating thermal and steady-state mechanical loads[45,46].

Conversely, TPS operates in a strictly nonlinear regime, with peak positive pressures reaching 25 MPa and microsecond rise times, dP/dt scales to 10^{13} Pa/s—five orders of magnitude greater than that of LIFU[13,21–25,33,47]. In this transient state, I_{spta} loses its dosimetric utility; a shockwave with a minimal duty cycle (e.g., 0.01%) but extreme peak gradients can trigger neuronal activation via instantaneous mechanical impulse, irrespective of its low time-averaged energy[18,21–23,34,39,40,48,49]. The efficacy of TPS is governed not by average power, but by the high-frequency harmonics ($f_{max} > 10$ MHz) generated through wavefront steepening[22,36,37,50–52]. To illustrate these fundamental differences in wave propagation, Figure 3 compares the time-domain pressure waveforms of linear LIFU, nonlinear LIFU with extreme peak sharpening, and the characteristic single-impact shock wave of TPS.

2.3 Momentum Transfer and the Volume Force Model

It is imperative to transition beyond the archaic "lithotripsy-based" destruction narrative[33,53–55]. Instead, TPS should be characterized by unidirectional momentum transfer facilitated by nonlinear absorption[26,28,29,31]. According to the Volume Force (F_v) model:

$$F_v = \frac{2\alpha I}{c}$$

where α represents the absorption coefficient, I denotes the instantaneous intensity, and c is the speed of sound. As the wavefront steepens, energy spectral density shifts toward high-frequency harmonics, where α increases quadratically (or near-quadratically) with frequency[20,26,41–43,56]. This mechanism results in a massive "injection" of momentum into the tissue on a nanosecond scale, generating a unidirectional mechanical impulse rather than symmetric oscillation[32,41,57–59]. At the cellular level, this impulse induces a high

displacement current ($i = V \cdot dC/dt$) across the neuronal membrane—a kinetic signature that is fundamentally distinct from the quasi-static deformation observed in LIFU[60–62,62–65]. (Table 3)

2.4 Diverging from the ITRUSST Framework

The physical idiosyncrasies necessitate the exclusion of TPS from the International Transcranial Ultrasonic Stimulation Safety and Standards (ITRUSST) reporting framework[45,46]. ITRUSST was fundamentally designed for quasi-continuous or long-pulse waves, with a primary focus on monitoring thermal index (TI) and steady-state cavitation[45,46,62,66,67]. Applying ITRUSST metrics to TPS is methodologically inconsistent, as time-averaged parameters inherently fail to capture the maximal mechanical impulse generated by transient nonlinear events[13,18,22,24,33,45,46]. Consequently, a physics-honest standard for TPS must prioritize ballistic parameters—specifically peak pressure gradients (dP/dt) and pulse energy-flux density (pEFD)—rather than metrics derived from thermodynamic equilibrium.

3. Mechanistic Divergence and Safety Assessments

3.1 LIFU: ARF and Bilayer Sonophores

LIFU-mediated neuromodulation is fundamentally anchored in steady-state mechanical coupling between the acoustic field and the cellular bilayer[58,59,62,66,68]. Unlike high-amplitude impulse techniques, LIFU employs a periodic ARF that exerts quasi-static pressure, effectively acting as a steady-state energy transducer [58,59,69]. This process is best elucidated by the Bilayer Sonophore (BLS) model, where cyclic pressure oscillations (0.5 MHz) drive intramembrane cavitation—periodic expansion and contraction of the intramembrane space [58,59,62,66,68,70]. These sub-micrometer dynamics modulate lipid bilayer

tension, thereby lowering the thermodynamic energy barrier for the gating of mechanosensitive ion channels, specifically the Piezo1 and TREK/TRAAK families [63–65,71–75]. From a translational perspective, the recruitment of TRPV4 channels in astrocytes suggests a neurovascular coupling pathway, potentially explaining the sustained functional connectivity changes observed in Alzheimer's pilot trials [6,63–65]. However, the transition from these biophysical micro-deformations to long-term clinical outcomes remains a critical gap requiring rigorous, sham-controlled validation.

3.2 TPS: The Impulsive Momentum Paradigm and Ballistic Gating Hypothesis

TPS represents a divergence from steady-state acoustics, operating instead on an impulsive momentum paradigm [33]. We propose a "Ballistic Gating" hypothesis to describe its unique mechanism: given that the ultra-short TPS pulse ($\approx 3\ \mu$s) is significantly faster than the viscoelastic relaxation time of neuronal membranes, the extreme pressure gradient ($dP/dt \approx 10^{13}$ Pa/s) delivers a localized mechanical impulse that bypasses slow-acting mechanotransductive pathways[61,76–78]. This transient stimulus induces a rapid oscillation of membrane capacitance (dC_m/dt), generating a substantial displacement current ($i = V \cdot dC/dt$) as characterized by the Neuronal Intramembrane Cavitation Excitation (NICE) model[62,68].

Although the Ballistic Gating hypothesis provides a physics-honest explanation for the rapid depolarization observed with TPS, direct validation in humans remains pending. Existing resting-state EEG and somatosensory evoked potential (SEP) studies have shown post-TPS changes in power spectra, coherence, and entropy, but these measurements lack the temporal resolution to capture the sub-millisecond displacement current transients induced by individual TPS pulses[18,38].

To rigorously substantiate the hypothesis and establish its mechanistic distinction from classic LIFU, we propose the following experimental roadmap performed in the same subjects under matched targeting and focal energy conditions: (i) high-density scalp EEG (⩾128 channels, sampling rate ⩾10 kHz) or MEG with real-time pulse triggering and advanced artifact suppression to compare time-locked evoked responses—specifically the latency, amplitude, and waveform of displacement-current-mediated transients (expected sub-millisecond for TPS) versus the slower oscillatory modulation induced by LIFU ARF (tens to hundreds of milliseconds)[21,79–81]; (ii) simultaneous ultrafast functional ultrasound (fUS) neuroimaging to co-register local hemodynamic responses and disentangle neuronal from vascular contributions between the two modalities[82,83]; (iii) in ethically approved cohorts already undergoing intracranial EEG (iEEG/SEEG) for clinical indications, opportunistic recording of local field potentials and multi-unit activity during interleaved TPS and LIFU sessions at the same cortical target[84,85]; and (iv) complementary ex vivo human brain-slice patch-clamp recordings to directly quantify capacitive versus mechanosensitive ion channel currents under matched acoustic parameters of both techniques[86,87].

3.3 Safety Assessment: The Biomechanical Boundary of Momentum Transfer

A fundamental paradox in TPS involves the efficient delivery of extreme acoustic momentum without inducing microstructural damage to the cerebral parenchyma. The resolution to this challenge lies in the nonlinear viscoelasticity of brain tissue[41,62,76,88,89].

Under the extreme strain rates ($\dot{\epsilon} > 10^5\ s^{-1}$) characteristic of TPS, the tissue undergoes a rapid transition from a dissipative fluid-like state to a solid-like regime. Within

this transient timescale, the shear modulus approaches its high-frequency limit G_∞, effectively entering a glassy regime[43,76,88,89]. This high-strain-rate stiffening ensures that the acoustic momentum is coupled into localized elastic work—sufficient to trigger ballistic channel gating—rather than being dissipated into destructive shear flow or inducing significant viscous heating[76,88–90].

This stiffening-mediated coupling constitutes the physical foundation of the exceptional safety profile of TPS, maximizing mechanotransductive efficiency while maintaining structural integrity[41,90]. However, this safety remains context-dependent; in the presence of anatomical instabilities within the targeted region, therapeutic mechanical impulses may transition into risks of structural compromise[90–96].

3.3.1 Vascular Fragility: The Failure of Brittle Structures

In pathological environments characterized by Cerebral Amyloid Angiopathy (CAA) and severe white matter hyperintensities (Fazekas Grade 3), the viscoelastic properties of the vascular wall undergo significant degradation[90,95–97]. The deposition of amyloid-beta within the tunica media replaces resilient smooth muscle fibers with rigid yet brittle structures, thereby impairing the vessel's capacity to buffer high-frequency acoustic impulses[23,98,99].

A Biophysical Model of Vascular Instability: Under the extreme pressure gradients characteristic of TPS ($dP/dt \approx 10^{13}$ Pa/s), tissues are subjected to a high-rate dynamic loading environment. We hypothesize that while healthy vasculature maintains structural integrity through transient elastic coupling, the compromised compliance of vessels affected by CAA predisposes them to mechanical failure. In this pathological state, the

inability of the brittle vascular wall to dissipate rapid acoustic energy may lead to an instantaneous exceedance of the Ultimate Tensile Strength (UTS) as the stress wave propagates, potentially triggering microvascular rupture. This theoretical framework provides a mechanistic rationale for the conservative exclusion of patients with pre-existing microbleeds in current clinical protocols[52,96,100–103].

Mechanistic Validation of Clinical Contraindications: From a biomechanical perspective, the classification of CAA, multiple cortical microbleeds, and severe small vessel disease as formal contraindications for ultrasound neuromodulation is highly rational[18,24,25,35,36,40,52,78]. Both the transient ballistic impulses characteristic of TPS and the sustained ARF inherent in LIFU represent potent mechanical triggers[8,37,104–106]. For the high-fragility vascular architectures observed in these pathologies, such energetic inputs pose a non-negligible risk of structural failure[94,100,103,107,108]. Our biophysical model thus provides a robust mechanistic justification for these established clinical safeguards, framing them not merely as empirical precautions but as essential protections against stress-induced vascular rupture.

3.3.2 The Therapeutic Gap: A Future Research Challenge

A significant proportion of the Alzheimer's disease population presents with concomitant vascular pathology. While current clinical screening protocols ensure safety by strictly excluding patients with suspected CAA, they inadvertently create a substantial therapeutic gap[4,6,7,9,11,22,23,50,109].

The primary challenge lies in engineering kinetic sub-threshold stimulation protocols specifically tailored for high-risk cohorts with vascular fragility. Future research must explore micro-pulse waveforms with enhanced harmonic coherence or develop acousto-

elasticity feedback systems capable of real-time monitoring of micro-strain responses within the vascular wall. Bridging the therapeutic access for this substantial sub-population is not merely a clinical ethics mandate; it represents the most formidable physical barrier for ultrasound neuromodulation to transcend from feasibility validation toward universal precision medicine[22,35,110].

As illustrated in Figure 4, the nonlinear TNUS regime offers a substantially wider biophysical window between neuromodulatory efficacy and vascular safety limits compared with quasi-linear LIFU. The clinical TPS operating point resides near the upper boundary of the glassy regime while still maintaining adequate safety margin even in vessels with compromised compliance.

4. Precision Dosimetry: From Standards to Feedback

4.1 Ballistic Metrics: A New Reporting Standard

Given the fundamental nonlinear kinetics established in Section 2, maintaining TPS within the conventional ITRUSST framework is no longer scientifically justifiable[18,33,45]. While linear metrics, such as I_{spta}, excel at monitoring the thermal indices of LIFU, they fail to capture the transient mechanical impulses that define TPS[12,45,70]. To bridge this dosimetric mismatch, we must pivot from time-averaged power toward ballistic parameters, establishing a reporting protocol specific to the nonlinear paradigm.

As a primary contribution of this review, we propose a minimum reporting list for TPS (Table 4). This framework is designed to provide a reproducible biophysical foundation for future clinical trials, ensuring complete physical honesty. Incorporating Fazekas scores or CAA status into the standardized reporting items signifies a paradigm shift from parameter-driven to structure-driven dosimetry. As demonstrated in Section 3.3,

any dosimetric characterization that neglects tissue integrity in patients with structural instabilities is inherently flawed. Mandatory reporting of vascular grading serves a dual purpose: it mitigates immediate clinical risk and facilitates the development of kinetic curves correlating pressure gradients with vascular tolerance. This evidentiary base ultimately paves the way for adaptive therapeutic pathways tailored for the high-proportion Alzheimer's sub-populations currently underserved due to the existing therapeutic gap.

4.2 Adaptive Compensation and Closed-Loop Titration

Future dosimetric standards must transition from static protocols to refraction-aware, adaptive systems[111]. The implementation of deep-learning solvers, inspired by TUSNet [112] could enable real-time acoustic field compensation with 21-ms latency. Adapting these end-to-end frameworks enables TPS systems to dynamically compensate for focal shifts induced by heterogeneous media—such as CSF-filled sulci—thereby optimizing targeting accuracy. Furthermore, integrating biophysical feedback—specifically EEG-derived oscillations or fMRI connectivity shifts—allows dosimetry to evolve from fixed-parameter stimulation into target-effect titration. This closed-loop architecture effectively bridges the disparity between nonlinear acoustics and clinical neurophysiology[13,19,49,113–115].

5. Clinical Audit: The JAMA RCT Analysis

The randomized clinical trial (RCT) published in 2025 provides a critical auditing point for TPS[35]. Although the study did not achieve statistical significance in its primary endpoint for the total population ($P = .68$), the age-interaction effect ($P = .003$) revealed a profound clinical stratification: the younger subgroup (≤ 70 years) demonstrated significant and sustained cognitive improvements in CERAD CTS scores, whereas the older subgroup (> 70 years) exhibited negligible benefits[35]. This heterogeneity is partially

attributed to the carryover effect inherent in the crossover design, where the therapeutic impact of the initial active phase persists into the second period, thereby diluting group differences.

From a biophysical perspective, a plausible contributing factor is the mismatch between biological brain age and physical energy distribution. While clinical discourse often attributes the diminished response in the elderly cohort to proteopathic burden or neurodegenerative attrition, refractive fidelity may represent an important physical bottleneck. In advanced AD, pathological expansion of the CSF compartment functions as a low-impedance refractive aberrator, driven by the acoustic velocity mismatch at the CSF–parenchyma interface ($c_{CSF} \approx 1500$ m/s vs. $c_{brain} \approx 1550$ m/s)[23,88,116]. According to Snell's law, the increased depth and heterogeneous geometry of sulcal CSF in atrophied brains induce substantial phase aberrations[116](Figure 5).

Critically, the TPS focal zone exhibits a mirrored-meniscus geometry—a direct spatial manifestation of its ultrashort pulse duration[12]. In this temporal regime, the transverse width of the impulse significantly exceeds its axial extent, rendering the focal spot exceptionally sensitive to lateral refractive shifts. Computational models confirm that CSF expansion in atrophied brains induces millimeter-scale focal displacements at the CSF–parenchyma interface, an effect that applies to both linear LIFU and nonlinear TPS in their current single-element implementations[12,19,20]. However, due to its narrow mirrored-meniscus focal geometry versus the larger elliptical profile of LIFU, TPS exhibits substantially greater refractive vulnerability to phase aberrations[12]. In younger patients with preserved brain volume, wavefront integrity remains robust. Conversely, in pronounced atrophy, the wavefront may undergo fragmentation and momentum dilution,

potentially causing the in situ mechanical impulse to fall below the activation threshold for mechanosensitive ion channels and thereby limiting nonlinear mechanotransduction[117,118].

The observed heterogeneity may also reflect baseline cognitive reserve, concomitant pharmacotherapy, or other unmeasured clinical confounders, underscoring the need for stratified randomization and covariate-adjusted analyses in future trials[35].

Despite the age-dependent variance in clinical scores, the fMRI data from the randomized clinical trial provide direct evidence for the underlying mechanisms of TPS: active stimulation significantly upregulated activation within core memory networks—specifically the precuneus and parahippocampal gyrus—and enhanced functional connectivity within the dorsal attention network[35]. These findings suggest that when acoustic energy effectively bypasses anatomical barriers, TPS can precisely modulate cognitive circuits[21–24,33,52].

6. Future Directions

The reclassification of TPS as TNUS necessitates a systematic realignment of research trajectories. To address the therapeutic gap identified in Section 3.3.2, the field must transition toward an integrated framework of hardware optimization, patient-specific modeling, and biological synergies.

6.1 Hardware Optimization: High-Density Phased Arrays and Adaptive Beamforming

The primary physical barrier in treating advanced AD remains the refractive aberration induced by CSF expansion and sulcal heterogeneity[22,23,35,36,52,114]. Current single-element systems lack the adaptive capacity to compensate for the focal shifts caused

by these high-impedance interfaces[18,34,39,40,49,50]. Future TPS platforms must prioritize high-density phased arrays to enable real-time wavefront correction[19,27,77,117,119]. By integrating deep-learning solvers such as TUSNet, these systems can perform end-to-end phase compensation with sub-30ms latency, neutralizing aberrations prior to shock-front steepening[112]. This computational transparency ensures that even in atrophied brains, peak pressure gradients (dP/dt) are maintained with millimetric precision within target cognitive hubs, such as the precuneus or entorhinal cortex[117,120,121].

6.2 Personalized Dosimetry: Structure-Aware Parameter Titration

Standardized stimulation parameters fail to account for the substantial anatomical variability in AD populations[9,122]. We advocate for a dynamic dosimetry model that calibrates acoustic energy based on a patient's structural impedance profile. This profile integrates (1) the atrophy-refraction index, derived from voxel-based morphometry, and (2) the vascular fragility map, based on Fazekas grading and susceptibility-weighted imaging (SWI). Under this framework, the TPS pulse sequence is transformed from a fixed output into an impulse-titrated parameter set. For younger patients with robust tissue elasticity, the system maximizes dP/dt to drive synaptic plasticity; for older patients with microvascular compromise, the system employs micro-pulse trains to optimize harmonic coherence while remaining below the ultimate tensile strength UTS of the vascular wall[11,23,123–126].

7. Conclusion

This perspective review demonstrates that the future of ultrasound neuromodulation depends on a fundamental shift from empirical observation toward deterministic, structure-

aware physical precision. Conventional dosimetric standards based on linear acoustic metrics, such as spatial-peak temporal-average intensity, are inadequate for characterizing the therapeutic mechanisms of TPS. By reclassifying TPS as TNUS, we identify its defining biophysical signature as the extreme pressure gradient and the resulting ballistic gating of mechanosensitive ion channels, a process governed strictly by the nonlinear Westervelt regime.

This mechanistic framework provides a biophysical basis for interpreting the age-dependent efficacy observed in recent clinical trials. In advanced Alzheimer's disease, pathological expansion of the cerebrospinal fluid compartment induces refractive aberrations that compromise wavefront integrity and focal targeting, particularly for the narrow mirrored-meniscus geometry characteristic of TPS. These findings suggest that refractive failure may contribute to the reduced response in older cohorts, beyond proteopathic or neurodegenerative factors alone.

To bridge this therapeutic gap, the field must transition toward structure-aware dosimetry. The integration of high-density phased arrays with physics-based deep-learning solvers, such as TUSNet, offers a pathway for real-time wavefront correction. By incorporating voxel-based morphometry and vascular fragility mapping, TPS protocols can evolve into individualized, impulse-titrated regimens that maximize efficacy in younger patients while maintaining mechanical stress below the ultimate tensile strength of compromised vessels in high-risk populations. Ultimately, recognizing the aging brain as a complex aberrating medium is essential for advancing ultrasound neuromodulation from empirical approximation toward reproducible clinical precision.

Disclosure

The authors declare that they have no known competing financial interests or personal relationships that could have appeared to influence the work reported in this paper.

Funding

This study was supported by Science and Technology Projects of Xizang Autonomous Region, China (Grant No.XZ202501ZY0120), National Scientific and Technological Innovation 2030 of China- Major Project (2023ZD0505300, 2023ZD0505304), General Program of Natural Science Foundation of Sichuan Provincial Department of Science and Technology (grant No.2024NSFSC0564, 2025ZNSFSC0730), and Grant (GYYX24005) from 1·3·5 Project of Center for High Altitude Medicine, West China Hospital, Sichuan University.

References

1. Honig LS, Sabbagh MN, van Dyck CH, et al. Updated safety results from phase 3 lecanemab study in early Alzheimer's disease. *Alzheimers Res Ther*. 2024;16(1):105. doi:10.1186/s13195-024-01441-8

2. van Dyck CH, Swanson CJ, Aisen P, et al. Lecanemab in Early Alzheimer's Disease. *N Engl J Med*. 2023;388(1):9-21. doi:10.1056/NEJMoa2212948

3. Jeong H, Im JJ, Park JS, et al. A pilot clinical study of low-intensity transcranial focused ultrasound in alzheimer's disease. *Ultrasonography*. 2021;40(4):512-519. doi:10.14366/usg.20138

4. Beisteiner R, Lozano A, Di Lazzaro V, George MS, Hallett M. Clinical recommendations for non-invasive ultrasound neuromodulation. *Brain Stimulation*. 2024;17(4):890-895. doi:10.1016/j.brs.2024.07.013

5. Nicodemus NE, Becerra S, Kuhn TP, et al. Focused transcranial ultrasound for treatment of neurodegenerative dementia. *Alzheimers Dement (N Y)*. 2019;5:374-381. doi:10.1016/j.trci.2019.06.007

6. Shimokawa H, Shindo T, Ishiki A, et al. A pilot study of whole-brain low-intensity pulsed ultrasound therapy for early stage of alzheimer's disease (LIPUS-AD): A randomized, double-blind, placebo-controlled trial. *The Tohoku Journal of Experimental Medicine*. 2022;258(3):167-175. doi:10.1620/tjem.2022.J078

7. Jeong H, Kim D, Na S, et al. Repeated neuromodulation with low-intensity focused ultrasound in patients with Alzheimer's disease. *Journal of Alzheimer's Disease*. 2025;105(3):955-965. doi:10.1177/13872877251333614

8. Jeong H, Song IU, Chung YA, et al. Short-Term Efficacy of Transcranial Focused Ultrasound to the Hippocampus in Alzheimer's Disease: A Preliminary Study. *Journal of Personalized Medicine*. 2022;12(2):2. doi:10.3390/jpm12020250

9. Fuh JL, Wang SJ, Wang PN, et al. Safety and efficacy of transcranial ultrasound stimulation for the treatment of Alzheimer's disease: A randomized, double-blind, placebo-controlled trial. *Ultrasonics*. 2026;159:107844. doi:10.1016/j.ultras.2025.107844

10. Huang SY, Wu MT, Sun CF, Yang FY. Volume Changes in Brain Subfields of Patients with Alzheimer's Disease After Transcranial Ultrasound Stimulation. *Diagnostics (Basel)*. 2025;15(3):359. doi:10.3390/diagnostics15030359

11. Ye BS, Chang KW, Kang S, Jeon S, Chang JW. Repetitive and extensive focused ultrasound–mediated bilateral frontal blood-brain barrier opening for alzheimer's disease. *Journal of Neurosurgery*. Published online January 1, 2025:1-8. doi:10.3171/2024.8.JNS24989

12. Truong DQ, Thomas C, Hampstead BM, Datta A. Comparison of Transcranial Focused Ultrasound and Transcranial Pulse Stimulation for Neuromodulation: A Computational Study. *Neuromodulation: Technology at the Neural Interface*. 2022;25(4):606-613. doi:10.1016/j.neurom.2021.12.012

13. Mitterwallner M, Matt E, Chen R, Beisteiner R. Ultrasound neuromodulation as a novel dementia therapy-Investigation of possible long-term confounds. *Alzheimers Dement (N Y)*. 2026;12(1):e70198. doi:10.1002/trc2.70198

14. Șovrea AS, Boșca AB, Dronca E, et al. Non-Drug and Non-Invasive Therapeutic Options in Alzheimer's Disease. *Biomedicines*. 2025;13(1):84. doi:10.3390/biomedicines13010084

15. Radjenovic S, Dörl G, Gaal M, Beisteiner R. Safety of clinical ultrasound neuromodulation. *Brain Sci*. 2022;12(10):1277. doi:10.3390/brainsci12101277

16. Sprick U, Günes AR, Beglau MV, Köhne M. Neuronavigated Transcranial Pulse Stimulation (TPS) with shock waves as a novel tool of noninvasive brainstimulation

(NIB) for a long-term treatment of Alzheimer's disease. *Eur Psychiatry*. 2025;68(Suppl 1):S252. doi:10.1192/j.eurpsy.2025.558

17. Cont C, Reinboth BS, Schütz C, et al. Transcranial Pulse Stimulation for Alzheimer's Patients. *JoVE*. 2025;(218):67176. doi:10.3791/67176

18. Beisteiner R, Matt E, Fan C, et al. Transcranial Pulse Stimulation with Ultrasound in Alzheimer's Disease-A New Navigated Focal Brain Therapy. *Adv Sci (Weinh)*. 2020;7(3):1902583. doi:10.1002/advs.201902583

19. Srivastav V, Puel J, Vappou J, Houten EV, Cabras P, Padoy N. A skull-adaptive framework for AI-based 3D transcranial focused ultrasound simulation. *arXiv*. Preprint posted online May 19, 2025:arXiv:2505.12998. doi:10.48550/arXiv.2505.12998

20. Slominski E, Marchant J, Judd W, et al. Influence of cerebrospinal fluid on power absorption during transcranial magnetic resonance-guided focused ultrasound treatment. *Med Phys*. 2023;50(6):3245-3257. doi:10.1002/mp.16427

21. Polte S, Klingmann L, Seßmann A, et al. Neuromodulatory effects of transcranial pulse stimulation (TPS) in neurological and psychiatric disorders—a systematic review and meta-analysis. *Neurology International*. 2025;17(11):188. doi:10.3390/neurolint17110188

22. Karakatsani ME, Gezginer I, Nozdriukhin D, et al. Transcranial pulse stimulation modulates neuronal activity and functional network dynamics. *Brain Stimulation: Basic, Translational, and Clinical Research in Neuromodulation*. 2025;18(6):1834-1842. doi:10.1016/j.brs.2025.09.021

23. Cont-Richter C, Stute N, Galli A, Schulte C, Wojtecki L. Transcranial Pulse Stimulation in Alzheimer's: Long-Term Feasibility and a Multifocal Treatment Approach. *Brain Sciences*. 2025;15(8):830. doi:10.3390/brainsci15080830

24. Wojtecki L. Commentary: Treating Diseases from Alzheimer's to Parkinson's Using Transcranial Pulse Stimulation: Mechanistic Insights, Recent Evidence, and Ethical Considerations. *NeuroSci*. 2025;6(2). doi:10.3390/neurosci6020056

25. Wojtecki L, Cont C, Stute N, Galli A, Schulte C, Trenado C. Electrical brain networks before and after transcranial pulsed shockwave stimulation in alzheimer's patients. *Geroscience*. Published online August 27, 2024. doi:10.1007/s11357-024-01305-x

26. Solovchuk M, Sheu TWH, Thiriet M. Simulation of nonlinear Westervelt equation for the investigation of acoustic streaming and nonlinear propagation effects. *The Journal of the Acoustical Society of America*. 2013;134(5):3931-3942. doi:10.1121/1.4821201

27. Dash PP, Arvanitis CD. Acoustic holography in the megahertz frequency range with optimal lens topologies and nonlinear acoustic feedback. *arXiv*. Preprint posted online August 24, 2025:arXiv:2508.07103. doi:10.48550/arXiv.2508.07103

28. Jing Y, Wang T, Clement GT. A k-Space Method for Moderately Nonlinear Wave Propagation. *IEEE Trans Ultrason Ferroelectr Freq Control*. 2012;59(8):1664-1673. doi:10.1109/TUFFC.2012.2372

29. Taraldsen G. A generalized Westervelt equation for nonlinear medical ultrasound. *J Acoust Soc Am*. 2001;109(4):1329-1333. doi:10.1121/1.1344157

30. Zemp RJ, Tavakkoli J, Cobbold RSC. Modeling of nonlinear ultrasound propagation in tissue from array transducers. *J Acoust Soc Am*. 2003;113(1):139-152. doi:10.1121/1.1528926

31. Rosnitskiy PB, Yuldashev PV, Sapozhnikov OA, Gavrilov LR, Khokhlova VA. Simulation of nonlinear trans-skull focusing and formation of shocks in brain using a fully populated ultrasound array with aberration correction. *J Acoust Soc Am*. 2019;146(3):1786-1798. doi:10.1121/1.5126685

32. Yuldashev PV, Khokhlova VA. Simulation of three-dimensional nonlinear fields of ultrasound therapeutic arrays. *Acoust Phys*. 2011;57(3):334-343. doi:10.1134/S1063771011030213

33. Wess O, Mayer J. The Interaction of Shock Waves With Biological Tissue - Momentum Transfer, the Key for Tissue Stimulation and Fragmentation. *International Journal of Surgery*. Published online February 27, 2025. doi:10.1097/JS9.0000000000002261

34. Cont C, Stute N, Galli A, et al. Retrospective real-world pilot data on transcranial pulse stimulation in mild to severe alzheimer's patients. *Front Neurol*. 2022;13:948204. doi:10.3389/fneur.2022.948204

35. Matt E, Mitterwallner M, Radjenovic S, et al. Ultrasound Neuromodulation With Transcranial Pulse Stimulation in Alzheimer Disease: A Randomized Clinical Trial. *JAMA Netw Open*. 2025;8(2):e2459170-e2459170. doi:10.1001/jamanetworkopen.2024.59170

36. Radjenovic S, Bender L, Gaal M, et al. A retrospective analysis of ultrasound neuromodulation therapy using transcranial pulse stimulation in 58 dementia patients. *Psychol Med*. 2025;55:e70. doi:10.1017/S0033291725000406

37. Beisteiner R, Matt E. Ultrasound neuromodulation - How deep can we stimulate? *Brain Stimul*. 2024;18(1):15-18. doi:10.1016/j.brs.2024.12.1189

38. Matt E, Kaindl L, Tenk S, et al. First evidence of long-term effects of transcranial pulse stimulation (TPS) on the human brain. *J Transl Med*. 2022;20(1):26. doi:10.1186/s12967-021-03222-5

39. Matt E, Dörl G, Beisteiner R. Transcranial pulse stimulation (TPS) improves depression in AD patients on state-of-the-art treatment. *Alzheimers Dement (N Y)*. 2022;8(1):e12245. doi:10.1002/trc2.12245

40. Popescu T, Pernet C, Beisteiner R. Transcranial ultrasound pulse stimulation reduces cortical atrophy in alzheimer's patients: A follow-up study. *Alzheimers Dement (N Y)*. 2021;7(1):e12121. doi:10.1002/trc2.12121

41. Parker KJ. Power laws prevail in ultrasound-tissue interactions. *Phys Med Biol*. 2022;67(9):10.1088/1361-6560/ac637e. doi:10.1088/1361-6560/ac637e

42. Payne A, de Bever J, Farrer A, Coats B, Parker DL, Christensen DA. A simulation technique for 3D MR-guided acoustic radiation force imaging. *Med Phys*. 2015;42(2):674-684. doi:10.1118/1.4905040

43. Maxwell A, Sapozhnikov O, Bailey M, et al. Disintegration of Tissue Using High Intensity Focused Ultrasound: Two Approaches That Utilize Shock Waves. *Acou Today*. 2012;8(4):24. doi:10.1121/1.4788649

44. Bader KB, Padilla F, Haworth KJ, et al. Overview of therapeutic ultrasound applications and safety considerations: 2024 update. *J Ultrasound Med*. 2025;44(3):381-433. doi:10.1002/jum.16611

45. Aubry JF, Attali D, Schafer ME, et al. ITRUSST consensus on biophysical safety for transcranial ultrasound stimulation. *Brain Stimulation*. 2025;18(6):1896-1905. doi:10.1016/j.brs.2025.10.007

46. Martin E, Aubry JF, Schafer M, Verhagen L, Treeby B, Pauly KB. ITRUSST consensus on standardised reporting for transcranial ultrasound stimulation. *Brain Stimulation: Basic, Translational, and Clinical Research in Neuromodulation*. 2024;17(3):607-615. doi:10.1016/j.brs.2024.04.013

47. Palacino F, Manganotti P, Benussi A. Targeting neural oscillations for cognitive enhancement in alzheimer's disease. *Medicina*. 2025;61(3):547. doi:10.3390/medicina61030547

48. Cheung T, Li TMH, Ho YS, et al. Effects of Transcranial Pulse Stimulation (TPS) on Adults with Symptoms of Depression-A Pilot Randomized Controlled Trial. *Int J Environ Res Public Health*. 2023;20(3):2333. doi:10.3390/ijerph20032333

49. Dörl G, Matt E, Beisteiner R. Functional specificity of TPS brain stimulation effects in patients with alzheimer's disease: A follow-up fMRI analysis. *Neurol Ther*. 2022;11(3):1391-1398. doi:10.1007/s40120-022-00362-8

50. Shinzato GT, Assone T, Sandler PC, et al. Non-invasive sound wave brain stimulation with transcranial pulse stimulation (TPS) improves neuropsychiatric symptoms in alzheimer's disease. *Brain Stimul*. 2024;17(2):413-415. doi:10.1016/j.brs.2024.03.007

51. Cont C, Stute N, Galli A, Schulte C, Logmin K, Wojtecki L. Long-term real world data on Transcranial Pulse Stimulation in Alzheimer's patients. *Brain Stimulation*. 2023;16(1):288. doi:10.1016/j.brs.2023.01.506

52. Karakatsani ME, Nozdriukhin D, Tiemann S, et al. Multimodal imaging of murine cerebrovascular dynamics induced by transcranial pulse stimulation. *Alzheimers Dement*. 2025;21(2):e14511. doi:10.1002/alz.14511

53. d'Agostino MC, Craig K, Tibalt E, Respizzi S. Shock wave as biological therapeutic tool: From mechanical stimulation to recovery and healing, through mechanotransduction. *International Journal of Surgery*. 2015;24:147-153. doi:10.1016/j.ijsu.2015.11.030

54. Simplicio CL, Purita J, Murrell W, Santos GS, Dos Santos RG, Lana JFSD. Extracorporeal shock wave therapy mechanisms in musculoskeletal regenerative medicine. *J Clin Orthop Trauma*. 2020;11(Suppl 3):S309-S318. doi:10.1016/j.jcot.2020.02.004

55. Wess OJ, Mayer J. Fragmentation of brittle material by shock wave lithotripsy. Momentum transfer and inertia: A novel view on fragmentation mechanisms. *Urolithiasis*. 2020;48(2):137-149. doi:10.1007/s00240-018-1102-6

56. Kyriakou A, Neufeld E, Werner B, Paulides MM, Szekely G, Kuster N. A review of numerical and experimental compensation techniques for skull-induced phase aberrations in transcranial focused ultrasound. *Int J Hyperthermia*. 2014;30(1):36-46. doi:10.3109/02656736.2013.861519

57. Khokhlova V, Fowlkes J, Roberts W, et al. Histotripsy methods in mechanical disintegration of tissue: Toward clinical applications. *Int J Hyperthermia*. 2015;31:1-18. doi:10.3109/02656736.2015.1007538

58. Tyler WJ, Lani SW, Hwang GM. Ultrasonic modulation of neural circuit activity. *Curr Opin Neurobiol*. 2018;50:222-231. doi:10.1016/j.conb.2018.04.011

59. Tyler WJ. Noninvasive neuromodulation with ultrasound? A continuum mechanics hypothesis. *Neuroscientist*. 2011;17(1):25-36. doi:10.1177/1073858409348066

60. Pasquinelli C, Hanson L, Siebner H, Lee H, Thielscher A. Safety of transcranial focused ultrasound stimulation: A systematic review of the state of knowledge from both human and animal studies. *Brain stimulation*. 2019;null:null. doi:10.1016/j.brs.2019.07.024

61. Gottlieb PA, Bae C, Sachs F. Gating the mechanical channel Piezo1. *Channels (Austin)*. 2012;6(4):282-289. doi:10.4161/chan.21064

62. Plaksin M, Kimmel E, Shoham S. Cell-type-selective effects of intramembrane cavitation as a unifying theoretical framework for ultrasonic neuromodulation. *eNeuro*. 2016;3(3):ENEURO.0136-15.2016. doi:10.1523/ENEURO.0136-15.2016

63. An W, Sun M, Zhang X, Huang L, Liu H, Cui B. Activation of Piezo1 and TRPV4 channels contributes to hCMEC/D3 cell mechano-sensing. *Front Physiol*. 2025;16. doi:10.3389/fphys.2025.1633251

64. Swain SM, Liddle RA. Piezo1 acts upstream of TRPV4 to induce pathological changes in endothelial cells due to shear stress. *J Biol Chem*. 2020;296:100171. doi:10.1074/jbc.RA120.015059

65. Liao WH, Hsiao MY, Kung Y, et al. TRPV4 promotes acoustic wave-mediated BBB opening via Ca2+/PKC-δ pathway. *J Adv Res*. 2020;26:15-28. doi:10.1016/j.jare.2020.06.012

66. Krasovitski B, Frenkel V, Shoham S, Kimmel E. Intramembrane cavitation as a unifying mechanism for ultrasound-induced bioeffects. *Proceedings of the National Academy of Sciences*. 2011;108(8):3258-3263. doi:10.1073/pnas.1015771108

67. Bae S, Liu K, Pouliopoulos AN, et al. Transcranial blood-brain barrier opening in Alzheimer's disease patients using a portable focused ultrasound system with real-time 2-D cavitation mapping. *Theranostics*. 2024;14(11):4519-4535. doi:10.7150/thno.94206

68. Tarnaud T, Joseph W, Martens L, Tanghe E. Computational modeling of ultrasonic subthalamic nucleus stimulation. *IEEE Trans Biomed Eng*. 2019;66(4):1155-1164. doi:10.1109/TBME.2018.2869042

69. Cox SS, Connolly DJ, Peng X, Badran BW. A Comprehensive Review of Low-Intensity Focused Ultrasound Parameters and Applications in Neurologic and Psychiatric Disorders. *Neuromodulation*. 2025;28(1):1-15. doi:10.1016/j.neurom.2024.07.008

70. Wynn Legon, Sato TF, Opitz A, et al. Transcranial focused ultrasound modulates the activity of primary somatosensory cortex in humans. *Nat Neurosci*. 2014;17(2):322-329. doi:10.1038/nn.3620

71. Lai A, Chen Y, Cox C, Jaworowski A, Peter K, Baratchi S. Analyzing the shear-induced sensitization of mechanosensitive ion channel Piezo-1 in human aortic endothelial cells. *Journal of cellular physiology*. 2020;236. doi:10.1002/jcp.30056

72. Beech DJ. PIEZO force sensing in vascular biology: An explosion of new knowledge, concepts and opportunity. *Adv Sci*. 2025;12(41):e11774. doi:10.1002/advs.202511774

73. Wijerathne TD, Ozkan AD, Lacroix JJ. Microscopic mechanism of PIEZO1 activation by pressure-induced membrane stretch. *J Gen Physiol*. 2023;155(5):e202213260. doi:10.1085/jgp.202213260

74. Choi D, Park E, Yu RP, et al. Piezo1-regulated mechanotransduction controls flow-activated lymphatic expansion. *Circ Res*. 2022;131(2):e2-e21. doi:10.1161/CIRCRESAHA.121.320565

75. Lin Y, Buyan A, Corry B. Computational studies of Piezo1 yield insights into key lipid–protein interactions, channel activation, and agonist binding. *Biophys Rev*. 2021;14(1):209-219. doi:10.1007/s12551-021-00847-0

76. Boiczyk GM, Pearson N, Kote VB, et al. Rate- and Region-Dependent Mechanical Properties of Göttingen Minipig Brain Tissue in Simple Shear and Unconfined Compression. *J Biomech Eng*. 2023;145(061004). doi:10.1115/1.4056480

77. Vanneste S, Reynolds J, De Ridder D. Focused transcranial ultrasound stimulation: A breakthrough approach to treating brain disorders. *Expert Rev Med Devices*. 2025;22(11):1231-1242. doi:10.1080/17434440.2025.2563618

78. Matt E, Radjenovic S, Mitterwallner M, Beisteiner R. Current state of clinical ultrasound neuromodulation. *Front Neurosci*. 2024;18:1420255. doi:10.3389/fnins.2024.1420255

79. Stango A, Zazio A, Barchiesi G, Bonfiglio NS, Bortoletto M. Impact of high-frequency sampling rate and stimulation intensity on early TMS artifacts: considerations for immediate TMS-EEG responses. *NeuroImage*. 2025;321:121526. doi:10.1016/j.neuroimage.2025.121526

80. Varone G, Hussain Z, Sheikh Z, et al. Real-Time Artifacts Reduction during TMS-EEG Co-Registration: A Comprehensive Review on Technologies and Procedures. *Sensors (Basel)*. 2021;21(2):637. doi:10.3390/s21020637

81. Hernandez-Pavon JC, Veniero D, Bergmann TO, et al. TMS combined with EEG: Recommendations and open issues for data collection and analysis. *Brain Stimul*. 2023;16(2):567-593. doi:10.1016/j.brs.2023.02.009

82. Bendig J, Aurup C, Blackman SG, McCune EP, Kim S, Konofagou EE. Transcranial Functional Ultrasound Imaging Detects Focused Ultrasound Neuromodulation Induced Hemodynamic Changes In Vivo. *bioRxiv*. Published online April 2, 2025:2024.03.08.583971. doi:10.1101/2024.03.08.583971

83. Kim S, Kwon N, Hossain MM, Bendig J, Konofagou EE. Functional ultrasound (fUS) imaging of displacement-guided focused ultrasound (FUS) neuromodulation in mice. *bioRxiv*. Published online April 1, 2024:2024.03.29.587355. doi:10.1101/2024.03.29.587355

84. Tsang EW, Tatz JR, Hassan U, et al. Transcranial magnetic stimulation with intracranial recording in humans and primates: a review. *Brain*. Published online November 18, 2025:awaf439. doi:10.1093/brain/awaf439

85. Papasavvas CA, Schroeder GM, Diehl B, Baier G, Taylor PN, Wang Y. Band power modulation through intracranial EEG stimulation and its cross-session consistency. *J Neural Eng*. 2020;17(5):054001. doi:10.1088/1741-2552/abbecf

86. Mesik L, Parkins S, Severin D, et al. Transcranial Low-Intensity Focused Ultrasound Stimulation of the Visual Thalamus Produces Long-Term Depression of Thalamocortical Synapses in the Adult Visual Cortex. *J Neurosci*. 2024;44(11):e0784232024. doi:10.1523/JNEUROSCI.0784-23.2024

87. Lee J, Tang Y, Roy A, Esfahani KS, Chang SY, Kim ES. Patch clamp recordings of action potentials from pyramidal neuron in hippocampus CA1 under focused ultrasound neurostimulation with MEMS self-focusing acoustic transducer. *J Neural Eng*. 2025;22(4):046004. doi:10.1088/1741-2552/ade7ae

88. Klemmer Chandía S, Schattenfroh J, Brinker ST, Tzschätzsch H, Sack I, Meyer T. Multimodal assessment of brain stiffness variation in healthy subjects using magnetic resonance elastography and ultrasound time-harmonic elastography. *Sci Rep*. 2024;14(1):28580. doi:10.1038/s41598-024-79991-y

89. Herthum H, Hetzer S, Kreft B, et al. Cerebral tomoelastography based on multifrequency MR elastography in two and three dimensions. *Front Bioeng Biotechnol*. 2022;10. doi:10.3389/fbioe.2022.1056131

90. Ventura-Antunes L, Nackenoff A, Romero-Fernandez W, et al. Arteriolar degeneration and stiffness in cerebral amyloid angiopathy are linked to aβ deposition and lysyl oxidase. *Alzheimers Dement*. 2025;21(6):e70254. doi:10.1002/alz.70254

91. Naydenov C, Manolova T, Mindov I. Alzheimer's Pathogenesis and Treatment by Transcranial Pulse Stimulation. *Open Access Maced J Med Sci*. 2023;11(F):206-209. doi:10.3889/oamjms.2023.11564

92. Scheltens P, Strooper BD, Kivipelto M, et al. Alzheimer's disease. *Lancet*. 2021;397(10284):1577-1590. doi:10.1016/S0140-6736(20)32205-4

93. Tayler H, Miners JS, Güzel Ö, MacLachlan R, Love S. Mediators of cerebral hypoperfusion and blood-brain barrier leakiness in Alzheimer's disease, vascular dementia and mixed dementia. *Brain Pathology*. Published online 2021. doi:10.1111/bpa.12935

94. Inoue Y, Shue F, Bu G, Kanekiyo T. Pathophysiology and probable etiology of cerebral small vessel disease in vascular dementia and Alzheimer's disease. *Mol Neurodegener*. 2023;18(1):46. doi:10.1186/s13024-023-00640-5

95. Charidimou A, Boulouis G, Frosch MP, et al. The Boston criteria version 2.0 for cerebral amyloid angiopathy: a multicentre, retrospective, MRI-neuropathology diagnostic accuracy study. *Lancet Neurol*. 2022;21(8):714-725. doi:10.1016/S1474-4422(22)00208-3

96. Hainsworth AH, Markus HS, Schneider JA. Cerebral Small Vessel Disease, Hypertension, and Vascular Contributions to Cognitive Impairment and Dementia. *Hypertension*. 2024;81(1):75-86. doi:10.1161/HYPERTENSIONAHA.123.19943

97. Fandler-Höfler S, Eppinger S, Ambler G, et al. Sex Differences in Frequency, Severity, and Distribution of Cerebral Microbleeds. *JAMA Netw Open*. 2024;7(10):e2439571. doi:10.1001/jamanetworkopen.2024.39571

98. Rezai AR, D'Haese PF, Finomore V, et al. Ultrasound blood–brain barrier opening and aducanumab in alzheimer's disease. *N Engl J Med*. 2024;390(1):55-62. doi:10.1056/NEJMoa2308719

99. Rezai AR, Ranjan M, D'Haese PF, et al. Noninvasive hippocampal blood-brain barrier opening in alzheimer's disease with focused ultrasound. *Proc Natl Acad Sci U S A*. 2020;117(17):9180-9182. doi:10.1073/pnas.2002571117

100. Zhang W, Liu Y, Kassab GS. Viscoelasticity reduces the dynamic stresses and strains in the vessel wall: Implications for vessel fatigue. *Am J Physiol Heart Circ Physiol*. 2007;293(4):H2355-2360. doi:10.1152/ajpheart.00423.2007

101. Hu HY, Ou YN, Shen XN, et al. White matter hyperintensities and risks of cognitive impairment and dementia: A systematic review and meta-analysis of 36 prospective studies. *Neurosci Biobehav Rev*. 2021;120:16-27. doi:10.1016/j.neubiorev.2020.11.007

102. Moretti R, Caruso P. Small Vessel Disease: Ancient Description, Novel Biomarkers. *Int J Mol Sci*. 2022;23(7):3508. doi:10.3390/ijms23073508

103. Lee DH, Lee EC, Park SW, Lee JY, Lee MR, Oh JS. Pathogenesis of Cerebral Small Vessel Disease: Role of the Glymphatic System Dysfunction. *Int J Mol Sci*. 2024;25(16):8752. doi:10.3390/ijms25168752

104. Yaakub SN, White TA, Roberts J, et al. Transcranial focused ultrasound-mediated neurochemical and functional connectivity changes in deep cortical regions in humans. *Nat Commun*. 2023;14(1):5318. doi:10.1038/s41467-023-40998-0

105. Qin PP, Jin M, Xia AW, et al. The effectiveness and safety of low-intensity transcranial ultrasound stimulation: A systematic review of human and animal studies. *Neuroscience & Biobehavioral Reviews*. 2024;156:105501. doi:10.1016/j.neubiorev.2023.105501

106. Beisteiner R, Hallett M, Lozano AM. Ultrasound neuromodulation as a new brain therapy. *Advanced Science*. 2023;10(14):2205634. doi:10.1002/advs.202205634

107. Li H, Jacob MA, Cai M, et al. Meso-cortical pathway damage in cognition, apathy and gait in cerebral small vessel disease. *Brain*. 2024;147(11):3804-3816. doi:10.1093/brain/awae145

108. Jacob MA, Cai M, van de Donk V, et al. Cerebral Small Vessel Disease Progression and the Risk of Dementia: A 14-Year Follow-Up Study. *Am J Psychiatry*. 2023;180(7):508-518. doi:10.1176/appi.ajp.20220380

109. Ham H, Kim KS, Lee JH, Kim DN, Choi HJ, Yoh JJ. Acoustic deep brain modulation: Enhancing neuronal activation and neurogenesis. *Brain Stimulation*. 2024;17(5):1060-1075. doi:10.1016/j.brs.2024.08.012

110. Legon W, Strohman A. Low-intensity focused ultrasound for human neuromodulation. *Nat Rev Methods Primers*. 2024;4(1):91. doi:10.1038/s43586-024-00368-6

111. Aubry JF, Bates O, Boehm C, et al. Benchmark problems for transcranial ultrasound simulation: Intercomparison of compressional wave models. *J Acoust Soc Am*. 2022;152(2):1003-1019. doi:10.1121/10.0013426

112. Naftchi-Ardebili K, Singh K, Popelka GR, Pauly KB. A deep-learning model for one-shot transcranial ultrasound simulation and phase aberration correction. *Med Phys*. 2026;53(1):e70259. doi:10.1002/mp.70259

113. Braun V, Blackmore J, Cleveland R, Butler CR. Transcranial ultrasound stimulation in humans is associated with an auditory confound that can be effectively masked. *Brain Stimulation*. 2020;13:1527-1534. doi:10.1016/j.brs.2020.08.014

114. Lo HKY, Fong TKH, Cheung T, et al. Enhanced cognition and modulation of brain connectivity in mild neurocognitive disorder: The promise of transcranial pulse stimulation. *Biomedicines*. 2024;12(9):2081. doi:10.3390/biomedicines12092081

115. Cheung T, Ho YS, Fong KH, et al. Evaluating the safety and efficacy of transcranial pulse stimulation on autism spectrum disorder: A double-blinded, randomized, sham-controlled trial protocol. *Int J Environ Res Public Health*. 2022;19(23):15614. doi:10.3390/ijerph192315614

116. Pham HQ, Nguyen N, Tran Q, Le TB, Le TQ. Efficient snell's law solution for generating robust acoustic tweezers in dual-layered media. *Front Acoust*. 2024;2. doi:10.3389/facou.2024.1485372

117. Llorente-Saguer I, Oxtoby NP. Enhanced monitoring of alzheimer's disease brain atrophy using composite value ratios of volumes. *Brain Commun*. 2025;8(1):fcaf497. doi:10.1093/braincomms/fcaf497

118. Chiarelli AM, Low KA, Maclin EL, et al. The optical effective attenuation coefficient as an informative measure of brain health in aging. *Photonics*. 2019;6(3):79. doi:10.3390/photonics6030079

119. Jamalabadi MYA. A Conservative Numerical Framework for Modeling Nonlinear Ultrasound Propagation in Thermoviscous Tissue Phantom. *Mathews Journal of Surgery*. 2025;8(2):1-11. doi:10.30654/MJS.10041

120. Gao R, Gao Y, Su W, Wang R. Decoding microglial polarization and metabolic reprogramming in neurodegenerative diseases: Implications for disease progression and therapy. *Aging and disease*. 2026;17(1):91-113. doi:10.14336/AD.2024.1629

121. Noel RL, Gorman SL, Batts AJ, Konofagou EE. Getting ahead of alzheimer's disease: Early intervention with focused ultrasound. *Front Neurosci*. 2023;17:1229683. doi:10.3389/fnins.2023.1229683

122. Frisoni GB, Hansson O, Nichols E, et al. New landscape of the diagnosis of Alzheimer's disease. *The Lancet*. 2025;406(10510):1389-1407. doi:10.1016/S0140-6736(25)01294-2

123. Mohammadjavadi M, Ash RT, Glover GH, Pauly KB. Optimization of MR acoustic radiation force imaging (MR-ARFI) for human transcranial focused ultrasound. *Magn Reson Med*. 2025;94(3):1060-1071. doi:10.1002/mrm.30539

124. Azaias C, Espert R, Montesinos MC, Khizroev S, Pardo M. Precision meets plasticity: Engineering and neurobiological frontiers of low-intensity focused ultrasound neuromodulation. *Preprints*. Preprint posted online November 17, 2025. doi:10.36227/techrxiv.176339151.16190371/v1

125. Jo Y, Kim S, Jeong J, Lee HJ. Ultrasound brain stimulation technologies for targeted therapeutics. *Nat Electron*. 2025;8(8):647-662. doi:10.1038/s41928-025-01420-3

126. Gupta S, Mudhafar M, Borole YD, Mahalakshmi V, Ramesh JVN, Khan MA. Optimizing transcranial focused ultrasound parameters: A methodological advancement in non-invasive brain stimulation for next-gen clinical applications. *Neurosci Inf*. 2025;5(2):100204. doi:10.1016/j.neuri.2025.100204

793 **Table 1. Abbreviations**

Abbreviation	Definition	Abbreviation	Definition
AD	Alzheimer's Disease	NICE	Neuronal Intramembrane Cavitation Excitation (Model)
Aβ	Amyloid-beta	RCT	Randomized Clinical Trial
BBB	Blood-Brain Barrier	SWI	Susceptibility-Weighted Imaging
BLS	Bilayer Sonophore (Model)	TI	Thermal Index
CAA	Cerebral Amyloid Angiopathy	TNUS	Transcranial Nonlinear Ultrasound Stimulation
CERAD CTS	Consortium to Establish a Registry for AD Cognitive Test Score	TPS	Transcranial Pulse Stimulation
CSF	Cerebrospinal Fluid	UTS	Ultimate Tensile Strength
EEG	Electroencephalography	TREK-1	Twik-Related Potassium Channel 1
Fazekas	Fazekas Scale (for white matter hyperintensities)	TREK-2	Twik-Related Potassium Channel 2
fMRI	Functional Magnetic Resonance Imaging	TRAAK	Twik-Related Arachidonic Acid-Activated Potassium Channel
ITRUSST	Int. Transcranial Ultrasonic Stimulation Safety and Standards	TRPV4	Transient Receptor Potential Vanilloid 4
LIFU	Low-Intensity Focused Ultrasound	Piezo1/2	Piezo-type Mechanosensitive Ion Channel Component 1/2

Abbreviation	Definition	Abbreviation	Definition
SEP	Somatosensory Evoked Potential	MEG	Magnetoencephalography
fUS	functional Ultrasound	iEEG	intracranial Electroencephalogram
SEEG	Stereoelectroencephalography		

794 **Table 2. Summary of Biophysical Symbols**

Symbol	Definition	Unit / Type	Symbol	Definition	Unit / Type
dP/dt	Peak pressure gradient	Pa/s	i	Displacement current	A
I_{spta}	Spatial-peak temporal-average intensity	W/cm^2	$f_{\max}$	Maximum harmonic frequency	MHz
F_v	Volume force	N/m^3	$\dot{\epsilon}$	Strain rate	s^{-1}
α	Absorption coefficient	Np/m	pEFD	Pulse energy-flux density	mJ/mm^2
I	Instantaneous intensity	W/m^2	Φ	Scalar potential	V
c	Speed of sound	m/s	∇	Del/Gradient operator	Operator
G_∞	High-frequency shear modulus	Pa	σ	Stress (Internal force)	Pa

Symbol	Definition	Unit / Type	Symbol	Definition	Unit / Type
C_m	Membrane capacitance	F/m^2	η	Dynamic viscosity	Pa · s

795

796

797 **Table 3. Biophysical Taxonomy and Mechanistic Divergence: LIFU vs. TPS (TNUS)**

Category	Biophysical Parameter	LIFU (Linear/Quasi-linear)	TPS / TNUS (Nonlinear/Impulsive)	Translational Implications
Acoustic Kinetics	Peak Pressure Gradient (dP/dt)	$\approx 10^8$ Pa/s (Low-gradient)	$\approx 10^{13}$ Pa/s (Shock-front)	Defines the transition from steady-state energy transduction to ballistic impulse.
	Wave Mechanics	Periodic sinusoidal oscillations	Nonlinear wavefront steepening	Nonlinear harmonics ($f_{max} > 10$ MHz) dominate energy deposition.
	Governing Equation	Linear Wave Equation	Westervelt Equation	Necessitates accounting for cumulative nonlinear distortion during propagation.
Tissue Rheology	Dynamic Coupling	Viscoelastic dissipative regime	High-strain-rate "Glassy" regime	Explains the safety profile: tissue stiffening converts momentum into elastic work, preventing shear damage.
	Interaction Modality	Acoustic Radiation Force (ARF)	Unidirectional Momentum Transfer	Shifts the focus from time-averaged push to instantaneous mechanical injection.
	Refractive Vulnerability	Low (Minimal phase aberration)	High (Sensitivity to CSF interfaces)	Critical for AD: explains focal shifts and efficacy loss in atrophied brains.
Cellular Dynamics	Biophysical Model	Bilayer Sonophore (BLS)	NICE Model / Ballistic Gating	Distinguishes between slow mechanical strain and rapid capacitive charging.

Category	Biophysical Parameter	LIFU (Linear/Quasi-linear)	TPS / TNUS (Nonlinear/Impulsive)	Translational Implications
	Primary Mechanism	Mechanosensitive channel gating	Displacement Current ($i = V \cdot dC/dt$)	Provides a physical basis for direct electrical activation via ultra-short pulses.
Dosimetric Standard	Framework Alignment	ITRUSST-compliant	Post-ITRUSST (Physics-honest)	I_{spta} is an obsolete metric for TPS; requires ballistic parameters (dP/dt, pEFD).
	Mandatory Reporting	I_{spta}, Duty Cycle, TI/MI	dP/dt, Pulse Rise Time, pEFD	Establishes a reproducible standard for nonlinear neuromodulation trials.

Notes and Definitions for Table 3:

- **Peak Pressure Gradient (dP/dt):** Represents the temporal steepness of the acoustic wavefront. The five-order-of-magnitude difference between LIFU and TPS marks the transition from linear mechanical oscillations to nonlinear shock-wave kinetics.
- **Westervelt Equation:** The governing equation for nonlinear acoustic propagation. Unlike the linear wave equation used for LIFU, it accounts for the cumulative harmonic distortion and energy redistribution that occur as TPS shock-fronts steepen during cranial penetration.
- **High-strain-rate "Glassy" Regime:** A biomechanical state where brain tissue transitions from a dissipative viscoelastic fluid to a solid-like elastic regime under extreme strain rates ($\dot{\epsilon} > 10^5$ s^{-1}). This stiffening effect ensures that acoustic momentum is coupled into elastic work (triggering ion channels) rather than being lost to destructive shear flow, explaining the high safety profile of TPS.
- **NICE (Neuronal Intramembrane Cavitation Excitation) Model:** A biophysical framework describing how acoustic energy induces intramembrane capacitive charging. In the context of TPS, it facilitates "**Ballistic Gating**," where the pulse is too rapid for conventional viscoelastic relaxation, leading to direct electrical depolarization.

- **Displacement Current ($i = V \cdot dC/dt$):** The current generated by the rapid change in membrane capacitance. This is the primary neurophysiological trigger for TPS, distinguishing it from the slower, strain-mediated mechanotransduction (e.g., Piezo1 gating) typically observed in LIFU.

- **Refractive Vulnerability:** The susceptibility of the acoustic focus to spatial shifting and energy dispersion. Nonlinear shockwaves are highly sensitive to the low-impedance interface of expanded cerebrospinal fluid (CSF) in atrophied brains, which induces phase aberrations that can lead to sub-threshold energy delivery at the intended target.

Table 4. Proposed Minimum Reporting List (MRL) for Transcranial Pulse Stimulation (TPS): A Hybrid Standard for Nonlinear Neuromodulation

The proposed MRL builds upon the ITRUSST framework by retaining its core safety indices (TI and MI) as a foundational layer while supplementing it with TNUS-specific ballistic and structural parameters. This hybrid approach ensures general safety screening, multi-center comparability, and clinical continuity while addressing the unique nonlinear mechanics of TPS.

Audit Dimension	*Core Reporting Parameters*	*Biophysical & Clinical Rationale*
1. Source Dynamics	• Thermal Index (TI) and Mechanical Index (MI) (retained from ITRUSST) • Peak Pressure Gradient ($\dot{P}$) & Rise Time (Δt_{rise}) • Pulse Energy Flux Density (pEFD) • Total Energy Load (TEL)	TI and MI provide essential general safety screening for thermal and cavitation risks, ensuring continuity with existing clinical practice. $\dot{P}$ and rise time define the impulsive momentum threshold critical for Ballistic Gating. pEFD serves as the primary dosimetric substitute for I_{SPTA}, quantifying instantaneous mechanical work. TEL monitors cumulative mechanical stress to prevent structural fatigue.

Audit Dimension	*Core Reporting Parameters*	*Biophysical & Clinical Rationale*
2. Structural Sensing	• Atrophy Grading (GCA Scale) • Neurovascular Status (Fazekas / CAA Grading)	Quantifies the "Refractive Barrier" and accounts for energy dispersion and focal shifts induced by expanded CSF interfaces. Defines the biomechanical "Red Line" for brittle, amyloid-laden vascular architectures under high $\dot{P}$.
3. Propagation Fidelity	• Focal Depth & Ray-Path Drift • Estimated In Situ Peak Negative Pressure (p^-) • Skull-Insertion Loss (dB) (retained from ITRUSST)	Corrects for spatial mismatch between nominal targeting and actual in situ energy deposition caused by tissue heterogeneity. Estimates effective intracranial pressure after frequency-dependent skull attenuation. Skull-insertion loss ensures compatibility with existing ITRUSST reporting.
4. Biological Verification	• Target-Effect Titration (EEG / fMRI)	Validates the successful translation of the physical impulse into a neurophysiological response (closed-loop verification).

Notes and Definitions for Table 4

- $\dot{P}$ **(Peak Pressure Gradient):** The maximum rate of pressure change during the rising phase of the acoustic pulse. In the TPS/TNUS regime, this value typically reaches 10^{13} Pa/s, serving as the definitive physical metric distinguishing nonlinear impulsive stimulation from quasi-linear periodic waves.
- Δt_{rise} **(Rise Time):** The temporal interval required for the pressure to increase from 10% to 90% of the peak positive pressure. An ultra-short rise time (microsecond scale) is essential for efficient momentum transfer before viscoelastic relaxation occurs in the neuronal membrane.

- **pEFD (Pulse Energy Flux Density):** The acoustic energy delivered per unit area per pulse (expressed in mJ/mm^2). Within the nonlinear framework, pEFD is mandated as the primary dosimetric substitute for I_{SPTA}.
- **TEL (Total Energy Load):** The cumulative mechanical energy exposure over a treatment session, calculated as pEFD $\times$ total pulse number. This metric is utilized to assess long-term tissue safety and structural fatigue limits.
- **GCA (Global Cortical Atrophy):** A clinical scale used to quantify the expansion of the cerebrospinal fluid (CSF) compartment. Due to sound speed heterogeneity and impedance mismatch, GCA scores serve as a structural proxy for predicting Ray-Path Drift.
- **Ray-Path Drift:** The physical phenomenon where the acoustic beam deviates from the nominal anatomical target due to refractive shifts at heterogeneous interfaces (e.g., expanded sulci).
- p^- **(In Situ Peak Negative Pressure):** The estimated intracranial peak negative pressure after correcting for frequency-dependent skull attenuation, reflection, and scattering (skull-insertion loss, typically reported in dB).
- **Target-Effect Titration:** The use of real-time neurophysiological feedback (e.g., EEG-evoked oscillations or fMRI functional connectivity shifts) to verify that the delivered physical impulse has surpassed the biological threshold for neuroplastic induction.

Figure legends

Fig. 1 | System architecture and operational principles of TPS and LIFU platforms

Both TPS and LIFU require an acoustic coupling hydrogel between the transducer and scalp to ensure efficient acoustic transmission. The TPS platform integrates optical tracking with a head-mounted guidance frame and handheld applicator, enabling real-time navigation relative to individual MRI anatomy. In contrast, modern LIFU systems employ frameless stereotactic navigation combined with infrared tracking to achieve precise alignment of the transducer with targeted brain regions. TPS delivers microsecond-scale pressure pulses (~3 μs duration), whose extremely brief duration—far shorter than that of LIFU—prevents any measurable temperature rise while producing spatially focused mechanical stimulation. Both systems incorporate real-time monitoring modules for acoustic output parameters to ensure procedural safety and reproducibility.

Fig. 2 | Comparative acoustic waveforms of LIFU and TPS stimulation paradigms

The schematic illustrates the contrasting waveform characteristics of theta-burst transcranial ultrasound stimulation (tbTUS, representing LIFU; Fig. 2A) and transcranial pulse stimulation (TPS; Fig. 2B). TPS generates monophasic high-pressure shock waves with an ultrashort 3 μs pulse width and nanosecond-scale rise time (peak pressure 10–100 MPa). The biphasic waveform comprises a brief compressive phase followed by a tensile wave and minor oscillations, producing mechanical bioeffects primarily via direct mechanotransduction and cavitation without thermal accumulation.

In contrast, tbTUS delivers 5 Hz pulse trains of 20 ms continuous-wave bursts, resulting in sustained neuromodulation accompanied by minor thermal and mechanical effects.

Fig. 3 | Comparative Acoustic Waveform Analysis: Linear vs. Nonlinear vs. TPS. Normalized pressure waveforms (time in microseconds) for three regimes. (1) Linear transcranial focused ultrasound (tFUS) exhibits smooth harmonic oscillation with periodic positive and negative phases. (2) Nonlinear tFUS shows extreme peak sharpening and high-harmonic saturation due to cumulative distortion. (3) TPS produces a single ultrashort impact pulse with a prominent positive pressure peak (p+) followed by a long rarefaction tail (p–) characteristic of viscoelastic recoil. These profiles highlight the transition from steady-state periodic forcing in LIFU to impulsive momentum transfer in TPS, directly supporting the proposed Ballistic Gating mechanism. Scale bar: 1 μs (horizontal).

Fig. 4 | Biophysical Windows: Efficacy Thresholds vs. Vascular Failure Limits

Peak pressure gradient ($\log_{10}$ scale) is plotted against neuromodulatory efficacy (precuneus activation relative to CERAD CTS percentage, left axis) and vascular safety margin (percentage of ultimate tensile strength, UTS, right axis). Blue curves represent quasi-linear LIFU; red curves represent nonlinear TNUS. The plot delineates the sharp efficacy increase once the system enters the high-strain-rate glassy regime, marks the clinical TPS operating point, and contrasts safety margins in healthy vasculature versus compromised vessels in cerebral amyloid angiopathy (CAA) with microbleeds. This

visualization underscores the distinct therapeutic window of TNUS and the necessity of structure-aware dosimetry in pathologically heterogeneous brains.

Fig. 5 | Impact of AD-related cortical atrophy on acoustic focal fidelity and spatial targeting

In healthy controls (left), the relatively uniform intracranial environment and minimal cerebrospinal fluid (CSF) layers allow for ideal focusing of TPS. This results in a high Focal Fidelity Index (FFI > 0.9), ensuring that the peak mechanical impulse is accurately delivered to the intended neural target. Conversely, in Alzheimer's disease (right), severe cortical atrophy creates widened CSF gaps that function as low-impedance refractive aberrators. The sound velocity mismatch at these expanded fluid-tissue interfaces induces significant phase aberrations, leading to focal collapse (energy smearing) and a lateral focal shift. This "refractive gap" causes the actual mechanical impulse to deviate from the planned target, potentially resulting in a sub-threshold dP/dt at the intended site and contributing to the age-dependent variance in clinical efficacy observed in recent trials.

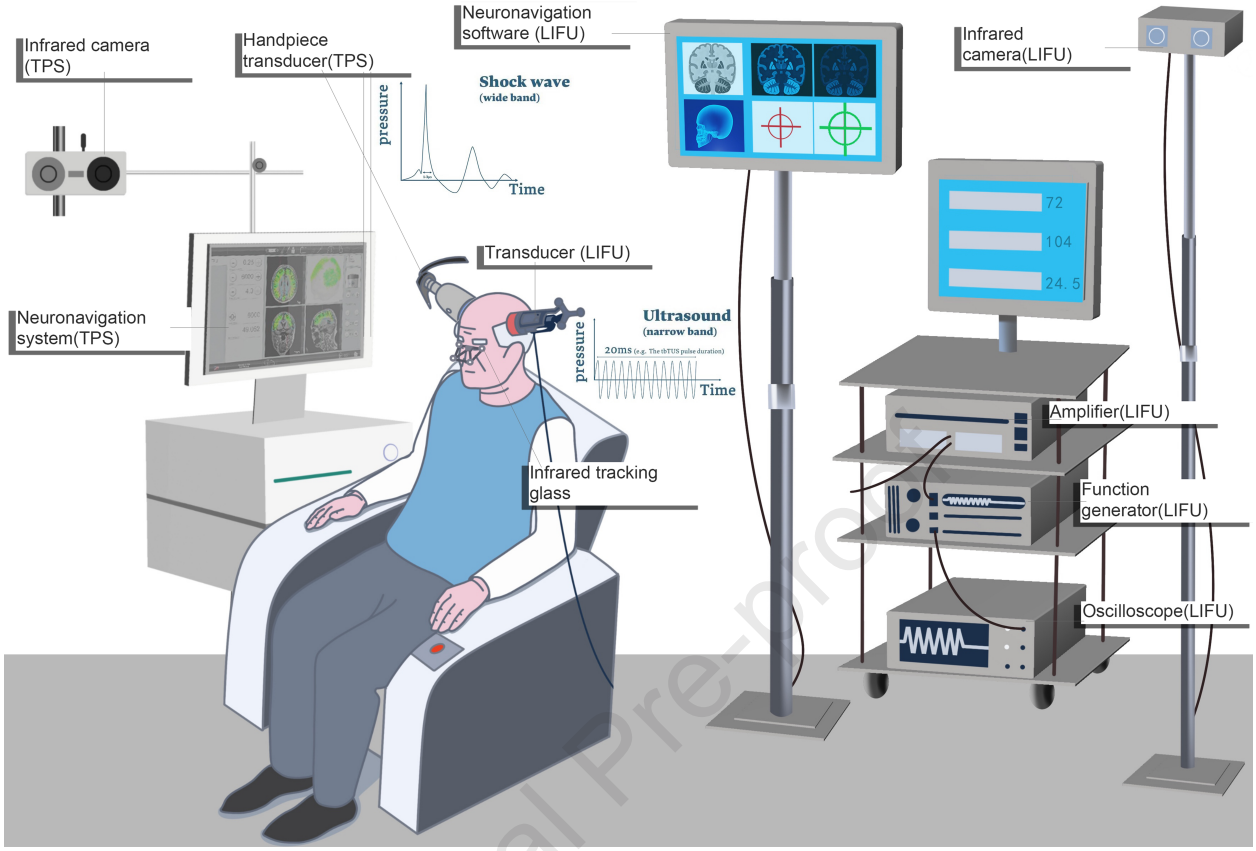

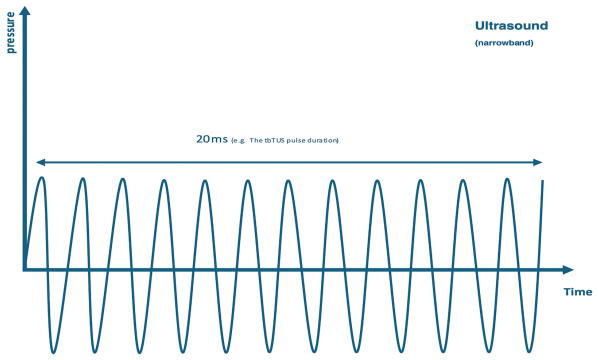

Figure 2A

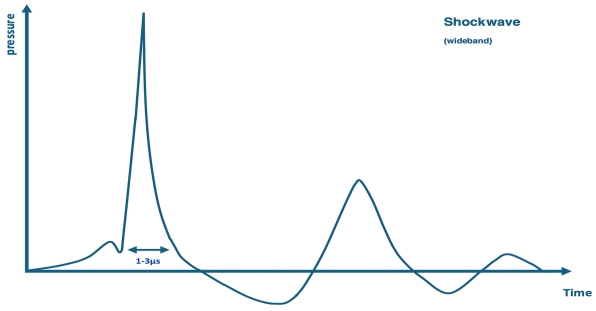

Figure 2B

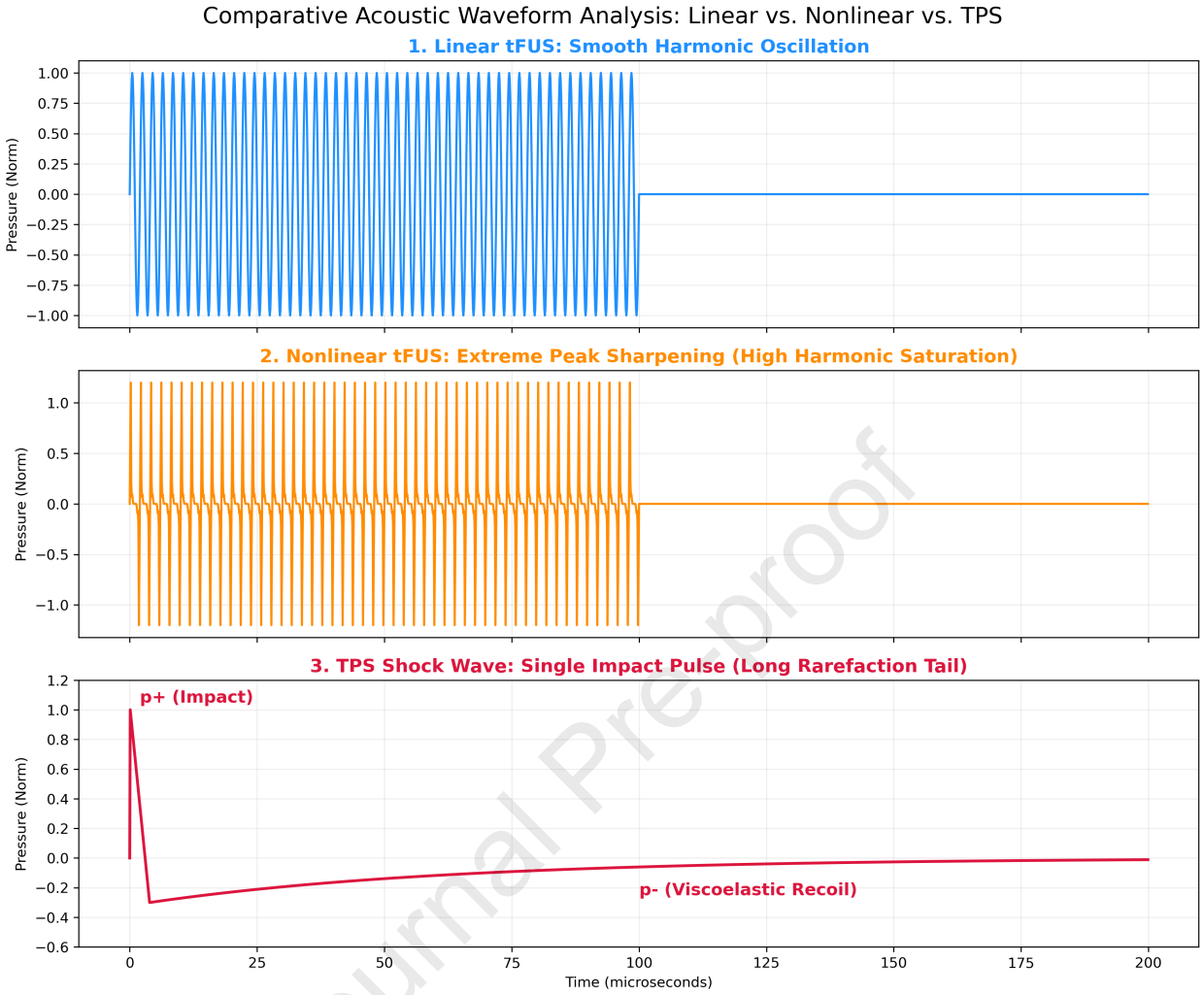

Figure 4. Biophysical Windows: Efficacy Thresholds vs. Vascular Failure Limits

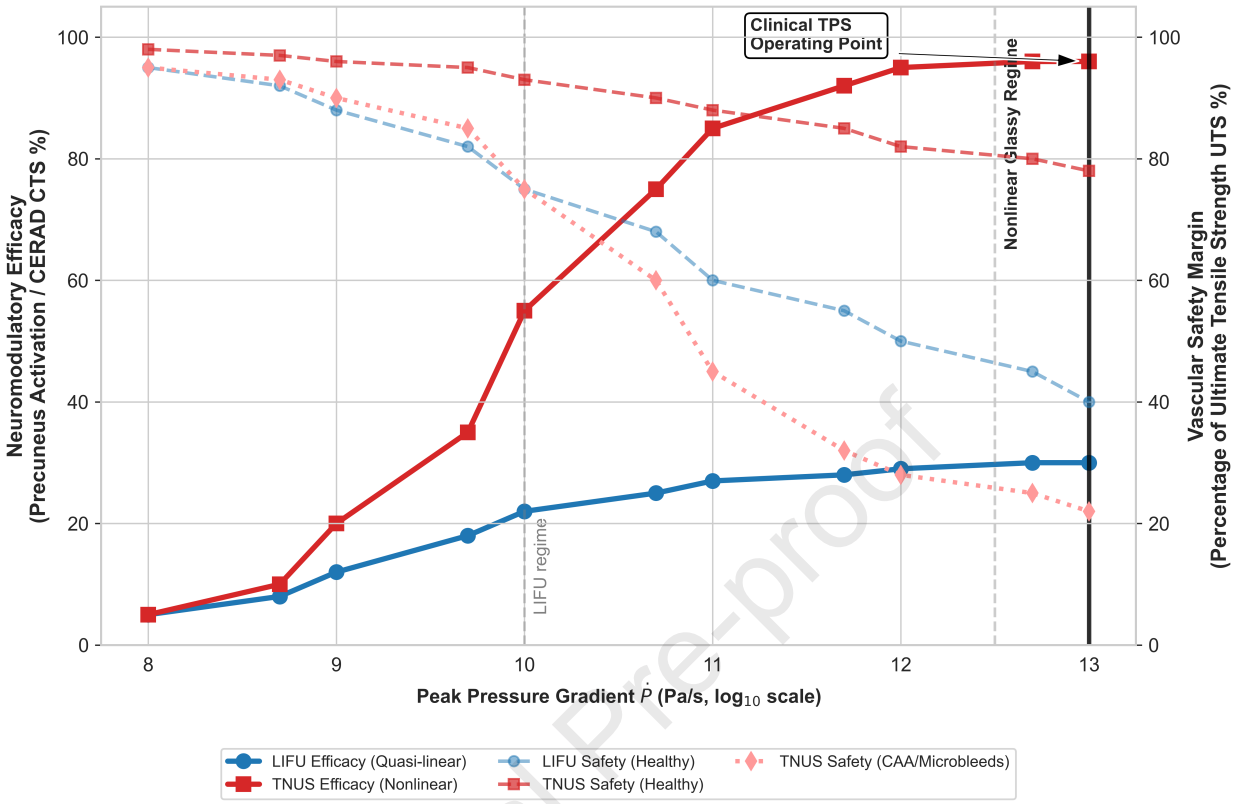

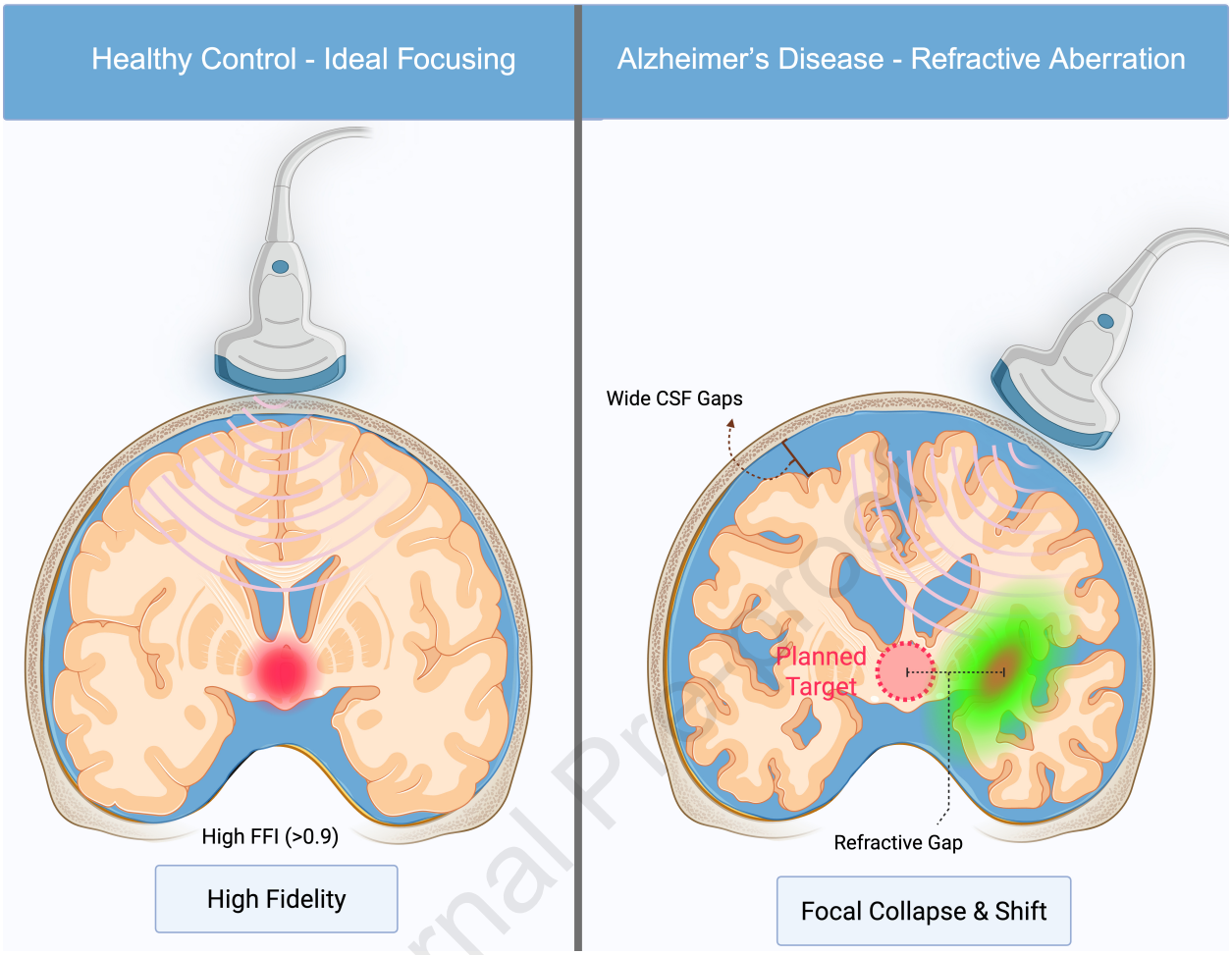

Declaration of interests

☒ The authors declare that they have no known competing financial interests or personal relationships that could have appeared to influence the work reported in this paper.

☐ The authors declare the following financial interests/personal relationships which may be considered as potential competing interests: